ACCELERATOR PHYSICS HIGHLIGHTS IN THE 1997/98 SLC RUN [*]

R.W. Assmann[†], K.L.F. Bane, T. Barklow, J.R. Bogart, Y. Cai, F.-J. Decker, J. Frisch,
R.H. Helm, L.J. Hendrickson, S.S. Hertzbach[‡], J. Irwin, R.K. Jobe, T. Kotseroglou,
P. Krejcik, S. Kuroda, D.J. McCormick, M.G. Minty, C.K. Ng, Y. Nosochkov, N. Phinney,
B. Podobedov, M.C. Ross, J.J. Russell, J. Safranek, D. Schulte[§], R.H. Siemann, G.V. Stupakov,
K.A. Thompson, J.L. Turner, T. Usher, C.X. Wang, D.H. Whittum, M.D. Woodley, Y.T. Yan,
and F. Zimmermann[¶], Stanford Linear Accelerator Center, Stanford, CA 94309

Abstract

We report various accelerator physics studies and improvements from the 1997/98 run at the Stanford Linear Collider (SLC). In particular, we discuss damping-ring lattice diagnostics, changes to the linac set up, fast control for linac rf phase stability, new emittance tuning strategies, wakefield reduction, modifications of the final-focus optics, longitudinal bunch shaping, and a novel spot-size control at the interaction point (IP).

1 DAMPING-RING LATTICE DIAGNOSTICS

In 1997 the South Damping Ring (SDR) optics was characterized by an analysis of the measured orbit response matrix with the program LOCO [1]. LOCO varies the individual gradients of the quadrupoles in a computer model (such as MAD [2]) to find the gradients that best reproduce the measured orbit response data.

Figure 1 compares the design optics for the SDR with the optics derived from a first statistical fit to the measured response matrices. The agreement was poor, and the χ^2 per degree of freedom was about 100. This plus the extreme variations in the fit model optics indicated some large systematic error. Subsequent inspection of the ring showed that the longitudinal locations of many beam-position monitors (BPMs) were not correct in the model. Once the model was updated, the LOCO calculation gave the more reasonable optics shown in Fig. 2 (left). The convergence of model-based ring orbit correction also improved.
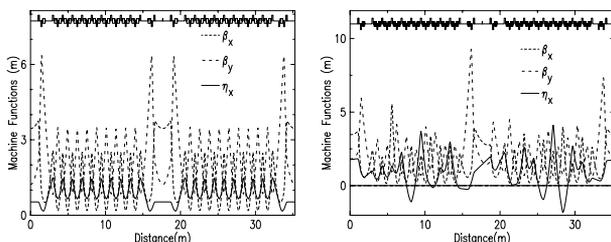
Figure 1: (Left) the design SDR optics; (right) optics according to the first analysis of the response matrix.
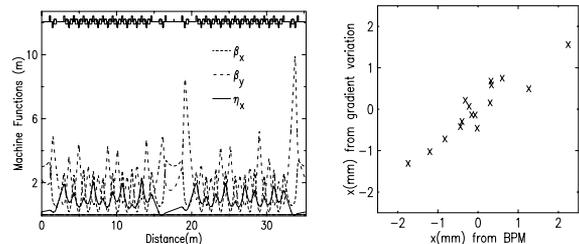
Figure 2: (Left) the SDR optics from fit to the response matrix after correcting the BPM position errors in the model; (right) the closed orbit at 16 QF magnets according to the BPMs and according to the variation in the fit gradients.

The optics in Fig. 2 (left) is still significantly different from the design optics. The model optics was fit to the measurements by only varying the gradients in the model quadrupoles, and assuming that the beam was centered in the sextupoles. Alternatively, we could also assume that the actual quadrupoles themselves have no gradient errors, and attribute the computed gradient variations entirely to orbit offsets in the adjacent sextupoles. In Fig. 2 (right), the orbit offsets so obtained are compared with the closed orbit measured at the BPMs adjacent to the 16 quadrupoles in the QF family. The good correlation indicates both that most of the calculated gradient error is caused by the orbit in the sextupoles and that the fit optics shown in Fig. 2 (left) is a reasonable representation of the true ring optics.

2 EMITTANCE TRANSPORT

In 1997, a variety of new techniques were adopted in order to preserve the small emittances from the damping rings. For example, the beam loss in the ring-to-linac transport line (RTL) was reduced by a new optics with larger momentum compaction factor [3], and a more robust lattice [4] improved the chromatic and wakefield-induced emittance dilution in the SLAC linac, while also ensuring compatibility with PEP-II (B factory) operation.

In previous years, one major source of linac instability had been the poor control over the rf phases, most notably over the phase reference of the 30 linac subboosters (each driving a group of 8 klystrons). In 1997, a fast subbooster phasing algorithm was implemented [5] by which the phases of all subboosters are measured within about 2 minutes. The energy variation induced by a $\pm 20°$ sub-

[†] Present address: CERN, SL, 1211 Geneva 23, Switzerland
[‡] University of Massachusetts, Amherst, Massachusetts 01003.
[§] CERN, PS, 1211 Geneva 23, Switzerland
[¶] Corresponding author

booster change is inferred from the orbit shift at high dispersion points in the beam switch yard (BSY) at the end of the linac. Fitting the observed dependence to a cosine function determines the subbooster phase with a resolution of about one degree S-band [5]. As an illustration of the new phasing method, Fig. 3 shows a measurement of the diurnal rf phase variation in different parts of the linac.
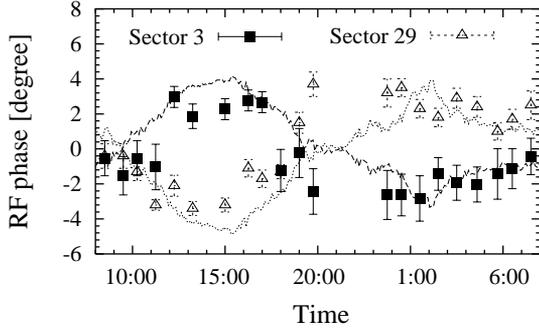
Figure 3: Measured diurnal variation of the RF phase error in degree S-band near the start (sector 3) and end (sector 29) of the linac. The opposite sign for sectors 3 and 29 is due to the fact that the phase of the injected beam is adjusted (for minimum energy spread at the end of the linac); the net phase change seen by the beam is therefore zero. The dashed lines represent an empirical correction derived from the outside temperature and the location along the linac [6, 7].

A second major breakthrough in linac operation was the routine application of two-beam dispersion-free steering [8]. Here, the absolute orbits of the electron and positron beams as well as their difference are minimized, while the strength of the orbit correctors is also restricted. In 1997, the dispersion-free orbit remained stable over several months, with only occasional reference-steering onto this orbit required to reestablish good emittances.

For the 1997/98 SLC run important changes were also implemented in the way the linac emittance is optimized [9]. Early in the linac, where the energy spread is large, the emittance growth is dominated by dispersion. In this region the orbit bumps introduced for emittance control [10] may generate additional wakefield tails. In the later parts of the linac the energy spread is small and wakefield-induced emittance dilution is more important. Tuning here has produced more stable results and lower emittances.

In the past, the emittances were optimized utilizing wire scanners located near but not at the end of the linac (after about 90% of its length). Simulations showed that emittance growth of up to 100% can occur in the last 10% [11]. For this reason, in 1997/98, wire scanners at the entrance to the final focus were used for emittance tuning. Figure 4 compares the rms variation of feedback setpoints which control the linac orbit bumps, in 1996 and 1997. The figure shows an overall reduction in setpoint variation as a result of the modified tuning strategy, and of the greater

orbit and rf phase stability. The improved emittances are documented by their average and rms values, in Table 1.
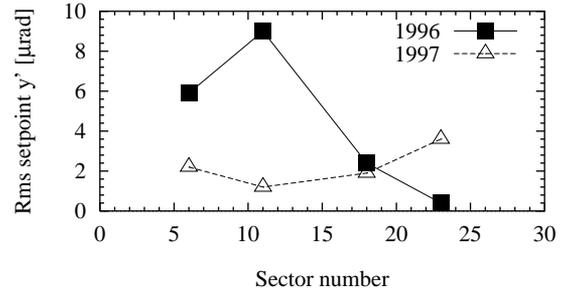
Figure 4: Rms variation of the vertical electron-orbit setpoints for 4 different feedback loops along the linac, over a three-month period in 1996 and in 1997.

	$\gamma\epsilon$ [10^{-5} m] (1996)				$\gamma\epsilon$ [10^{-5} m] (1997)			
	e^-		e^+		e^-		e^+	
	$\bar{\epsilon}$	σ_ϵ	$\bar{\epsilon}$	σ_ϵ	$\bar{\epsilon}$	σ_ϵ	$\bar{\epsilon}$	σ_ϵ
Li02 X	3.8	1.4	4.4	0.6	3.5	0.6	4.0	0.6
Li02 Y	0.5	0.1	0.3	0.1	0.5	0.4	0.3	0.1
Li28 X	5.5	1.8	5.7	2.1	4.5	0.7	5.1	1.1
Li28 Y	1.1	0.8	0.8	0.7	0.9	0.6	0.7	0.3
FF X	5.7	1.4	5.8	3.1	5.3	0.6	5.1	0.6
FF Y	2.1	1.2	1.3	0.8	1.3	0.4	0.9	0.2

Table 1: Average emittances ($\bar{\epsilon}$) and rms variation (σ_ϵ), measured at the entrance to the linac (Li02), close to its end (Li28) and in the final focus, for two three-month periods in 1996 and 1997.

3 WAKEFIELDS AND IP DIVERGENCE

Early in 1997 it was discovered that the movable collimators in the final focus were equipped with secondary-emission (SEM) blades whose original purpose was to detect beam loss and to assist in steering. The sharp-edge blades were estimated to almost triple the collimator wakefield [12], as seen in Fig. 5, and to increase the vertical IP spot size roughly by a factor 3–4 for a 2σ betatron oscillation [13]. The blades were removed prior to the 1997 run.

In 1997, the IP beta functions were squeezed by increasing the demagnification between the sextupoles and the IP. This optics change should also reducepotential dilutions caused by upstream wakefields or nonlinear aberrations. Improved background control [14] allowed operation with a horizontal IP angular divergence 30% larger than in 1996. The vertical divergence was similar to previous runs, albeit for a much smaller vertical emittance. Table 2 compares some IP parameters for 1996 and 1997.
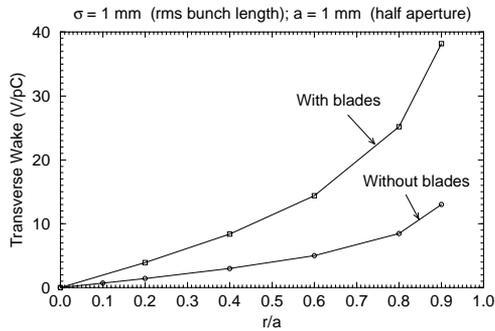
Figure 5: Calculated transverse wakefield kick from collimator jaws with and without SEM blades [12].

parameter	1996		1997	
	e^-	e^+	e^-	e^+
θ_x^* [μrad]	363	376	439	489
θ_y^* [μrad]	280	248	269	249
β_x^* [mm]	4.8	4.5	2.9	2.2
β_y^* [mm]	3.0	2.3	1.7	1.4

Table 2: Approximate average values of rms angular divergences and IP beta functions for electrons and positrons.

4 BUNCH SHAPING AND IP TUNING

The SLC luminosity depends on the longitudinal IP bunch distribution. Utilizing the momentum compaction of the arcs, this distribution can be varied by adjusting the net linac rf phase, as illustrated in Fig. 6.
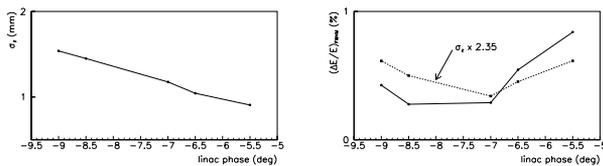
Figure 6: (Left) rms bunch length and (right) FWHM energy spread at the IP as a function of the beam phase with respect to linac rf crest [16]; the dotted line is the rms energy spread times 2.35.

Simulations with the code Guinea-Pig [15] show that a phase change of 3.5° causes a luminosity variation of about 20% [16]. The rf phase can be controlled using either the measured energy loss due to beamstrahlung or the signal of a newly installed rf bunch-length monitor [17]. The strong sensitivity to the linac rf phase could explain slow drifts, by up to 30%, in the ratio of the luminosity estimated from beam-beam deflection scans and the actual luminosity recorded by the SLD detector.

At the SLC, the IP spot size is optimized frequently by correcting the horizontal and vertical waist positions, dispersion and skew coupling for both beams. Until 1997, this optimization was performed by the operators using beam-beam deflection scans, a lengthy and inaccurate procedure.

In the 1996 run, the limited resolution of the deflection scans was estimated to be responsible for a 20-40% luminosity loss [18]. The situation was improved in 1997, when an automatic dithering feedback was implemented [19]; see Fig. 7. This feedback corrects the aberrations, one at a time, as needed. It uses the signal from a beamstrahlung monitor, which it correlates to step-up and step-down changes of actuators. The new feedback stabilizes the IP tuning and facilitates fast recovery after down periods.
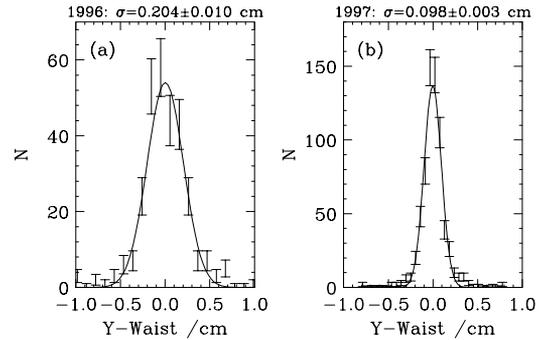
Figure 7: Distribution of incremental changes in the vertical waist position over a three month period (a) during the 1996 SLC run; (b) in the fall of 1997 [20].

5 CONCLUSION

The many new ideas described in this report demonstrate the continuing importance of the SLC for developing and understanding the techniques required for future linear colliders.

6 REFERENCES

[1] J. Safranek, Nucl. Instr. and Meth. A388, 27 (1997).

[2] H. Grote, F.C. Iselin, CERN/SL/90-13, 1991.

[3] S. Kuroda, SLAC CN-418; P. Raimondi, F. Zimmermann, unpublished (1997).

[4] Y. Nosochkov et al., unpublished (1997).

[5] J. Bogart et al., submitted to EPAC98.

[6] F.J. Decker et al.; R.W. Assmann et al., PAC97.

[7] K. Jobe, unpublished (1997).

[8] R. Assmann et al., submitted to EPAC98.

[9] R. Assmann, F.J. Decker, P. Raimondi, EPAC98.

[10] J.T. Seeman et al., Proc. HEACC'92, p. 879 (1992).

[11] R. Assmann, PAC97 Vancouver.

[12] C. Ng, unpublished (1997).

[13] F. Zimmermann et. al., EPAC96, p. 504 (1996).

[14] S. Hertzbach, T. Usher, P. Raimondi, unpubl. (1996/97).

[15] D. Schulte, unpublished (1993).

[16] F. Zimmermann et al., SLAC-CN-417 (1997).

[17] F. Zimmermann et al., PAC97 Vancouver (1997).

[18] P. Emma et. al., PAC97 Vancouver (1997).

[19] L. Hendrickson et al., ICALEPCS 1997.

[20] P. Emma, unpublished (1998).